ACTA STEREOL 1998; 17/1: 123-139
ORIGINAL SCIENTIFIC PAPER

Systematic Error of the Spherical Grain Model in Converting Grain Size Distributions and its Correction with the New Models

X. B. Zhao [1], K. Lücke [2]

1 : Department of Materials Science and Engineering, Zhejiang University, Hangzhou 310027, P.R. China

2 : Institut für Metallkunde und Metallphysik, RWTH Aachen, Kopernikusstr. 14, D-52056 Aachen, FRG

Abstract

Three-dimensional (3D) grain sizes were generally obtained by converting the 2D or 1D grain sizes to 3D with the methods based on spherical grain model (S-model). In this paper, the systematic error and its origin involving the conversion of grain sizes caused by the S-model is analyzed in the 2-D case, and a new polyhedral grain model (P-model) is developed to calculate 3D and 2D grain sizes from the 2D and/or 1D data. Experimental analyses show that the systematic error originated from the spherical model can be well corrected by using the new polyhedral model.

KEY WORDS : Grain size, geometric model, systematic error.

1. Introduction

One of the most important quantities to be determined in polycrystalline materials is the grain size distribution function (SDF). The grain size is defined with the volume V in three dimensional (3D) cases, or with the (intersect) area A in 2D, or the intercept length L in 1D of a grain. Mostly also an equivalent radius R is used as the grain size, which is defined as the radius of the sphere of equal volume in 3D or of a circle of equal area in 2D or as half the intercept length in 1D of the grain, respectively:

$$V = \frac{4}{3}\pi R_3^3; \qquad A = \pi R_2^2; \qquad L = 2R_1 \tag{1}$$

Where the dimension of grain is indicated with the subscript 1, 2 or 3 of R. Correspondingly, a SDF, $F(R)$ is defined so that $F(R)dR$ gives the relative number of grains (frequency) in the range between

R and $R+dR$ with $\int F(R)dR = 1$, or, in the discrete form, F_i gives the frequency of the grains in the i-th size class with $\sum_i F_i = 1$.

The problem which here arises stems from the fact that only the 1D and eventually also the 2D grain size can easily be measured, but that it is extremely laborious and for large style investigations practically impossible to experimentally determine the grain volume and thus the SDF for 3D grains (e.g. by continuous sectioning [1,2]). But, since mainly 3D bodies are used, it is just this 3D SDF which is the most important one. For this reason, procedures to reproduce the 3D SDF from a 1D or 2D distribution being obtained by measuring the intercept lengths along random straight lines or the intersect areas in random sections through the specimen were treated first by biologists[3] and later also by metallurgists (e.g. Scheil[4,5]) before about 70 years, which were all based on the supposition of spherical shaped grains, and so that were referred here to as "spherical grain model", i.e. S-model. The S-model is generally accepted and till now is the most popular method applied to obtain 3D grain size distributions. It is now our purposes (i) to show that this method will cause grave systematic errors in the converted SDFs and often does not give even a good approximation, and (ii) to present a way for deriving a more correct distribution.

The reproduction of a higher dimensional SDF $F(R)$ from a measured lower dimensional SDF $f(r)$ is based on the fundamental equation:

$$f(r) = \int q(R)p(R,r)F(R)dR \qquad (2)$$

Here $q(R)$ is the probability that a grain of size R is met by an arbitrary (measuring) section or straight line through the specimen (called as "sampling effect"), and $p(R,r)$ is the probability that such a section or line going through a grain with radius R leads to an area or intercept of radius r with $r \le R$ ("truncation effect"). However, q and p depend on the geometrical shape of the grains so that, for evaluating Eq.(2), a geometrical model of the grains must be assumed.

The only model generally accepted until now is, as just mentioned, the S-model, which has the advantage that the functions $q(R)$ and $p(R,r)$ can easily be derived. One obtains here for the 1D $\rightarrow$ 2D, 2D $\rightarrow$ 3D and 1D $\rightarrow$ 3D conversions[6]:

$$\begin{cases} q_{12}^{S}(R) = 2R \quad ; \quad p_{12}^{S}(R,r) = r \Big/ \left(R\sqrt{R^2 - r^2} \right) \\ q_{23}^{S}(R) = 2R \quad ; \quad p_{23}^{S}(R,r) = r \Big/ \left(R\sqrt{R^2 - r^2} \right) \\ q_{13}^{S}(R) = \pi R^2 \quad ; \quad p_{13}^{S}(R,r) = 2r/R^2 \end{cases} \tag{3}$$

After inserting these expressions into Eq.(2) the unknown function $F(R)$ can be calculated by inversion of this equation, if the distribution $f(r)$ is known (e.g. has been measured).

Since the first presentation of this method in 1925 [3], many papers have been published on this model (overviews are given by DeHoff [7] and Exner [6]). However, they all deal with secondary questions, as e.g. with another derivation of Eq.(3), with the better numerical solution of Eq.(2), with the statistical error caused by the division of grain sizes into discrete classes, or with the equation whether the application of 2D $\rightarrow$ 3D or 1D $\rightarrow$ 3D inversion will lead to better reproductions etc.[8~14] But only little attention has been given to the primary question of what is the error caused by the model itself, i.e. by the assumption of spherical and circular instead of polyhedral and polygonal grains. Naumovich *et al.*[15] have calculated the function $p(R,r)$ for a cube, a tetrahedron, a tetrakaidecahedron and a rhombic dodecahedron and found that the difference of the 3D SDFs reproduced from the intersect area (2D) distribution with various geometric models is much smaller than that reproduced from the intercept (1D) distribution. But in their paper the function $q(R)$ was not considered and no explicit practical method was given for the calculation of 3D SDFs using polyhedron models.

An indication of the error caused by the S-model gives already Fig. 1. For a grain pattern containing 780 grains copied from the micrograph of an annealed ordered NiAl sample (Fig.1a), the measured one-dimensional grain size distribution (1D GSD) and the 3D SDF derived from it by the

S-model (practically, Bockstiegel's method[9]) are plotted in Fig. 1b. One recognizes that this 3D SDF contains many small grains (grains with R<20μm amount to more than 50%), which do not show up in the micrograph and thus must be a result of an erroneous reproduction method ("ghost grains"). In Fig. 1b, another 3D SDF calculated with a new method called "DPF method" based on polyhedral grain model [16] is also plotted (dash-dot line), which, with the maximum probability of grain size at about 50 μm, seems to be much closer to the reality.

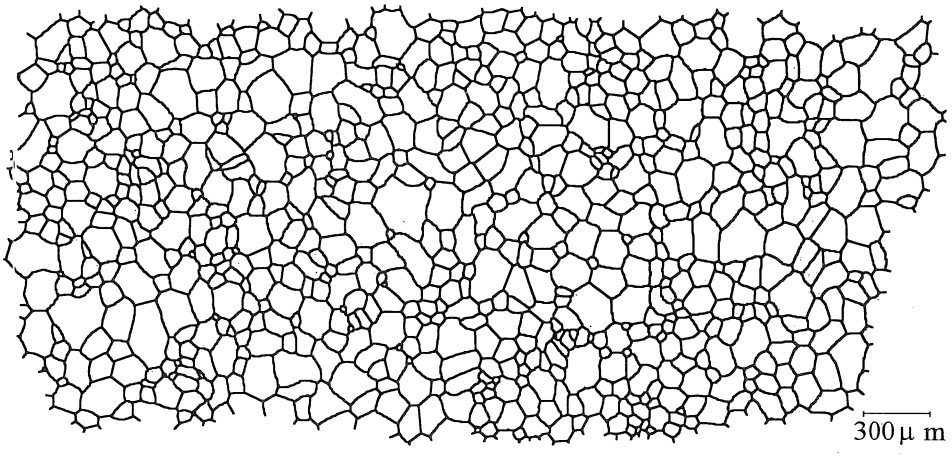

(a) grain pattern of a ordered NiAl polycrystalline sample

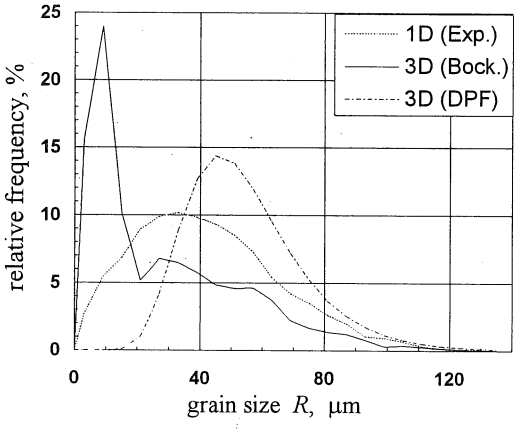

(b) 1D grain size distribution (dash line) measured from Fig.1a and the 3D SDF reproduced with S-model (solid line) and the DPF-method[16] based the polyhedral model (dash dot line).

Fig. 1 an example to show the systematic error of the S-Model

To discussion the origin of the error of S-model and to develop a new geometrical model by which a better approximation can be achieved, the reproduction of 2D SDFs from measured 1D data will be investigated in the next section. This problem —— because of its lower dimensionality —— is firstly simpler than the ones including 3D distributions, secondly has the advantage that both the 1D and 2D distributions can be measured and thus the validity of the model can be experimentally checked, and thirdly has the same principle as the conversion of 3D SDFs (e.g. the 2D→3D conversion has the same q and p functions as the 1D→2D conversion in the S-model). And then, in Section 3, we well discuss the conversion of 3D SDFs.

2. Origin of the error of the S-model and the development of the P-model

In order to demonstrate the main difference between the S-model applying circular grains and a real microstructure consisting of polygonal grains, a subfield of the grain pattern of Fig. 1a with 28 grains is redrawn in Fig. 2 a and the grains are replaced in Fig. 2b with circles of the same sizes. Then the 1D grain size distribution (GSD) as well as the 1D circle size distribution (CSD) have been derived by laying straight lines through the patterns and plotted in Fig. 2c.

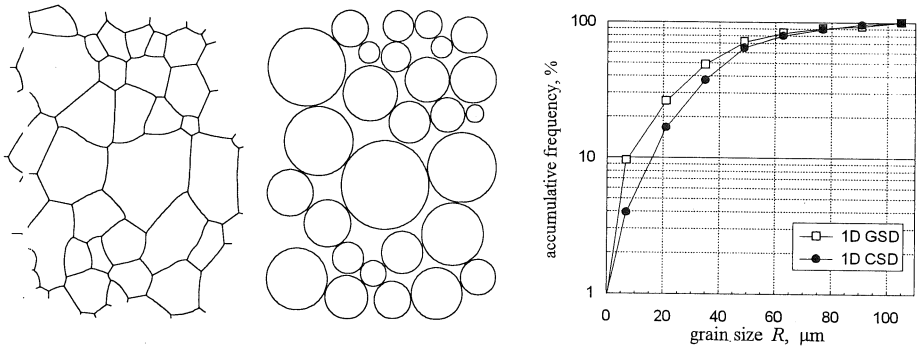

(a) grain pattern (b) area-equal circles (c) 1D SDF measured from the grain pattern and the circle pattern

Fig. 2 an example to show the difference between polygonal and circular grains

One sees in Fig. 2c that the 1D size distributions measured from the grain pattern and the circle pattern are very different, particularly for the small intercepts. Since Fig. 2b has the same geometrical feature as the S-model, this means that using the S-model one could obtain the *true* 2D SDF only from the 1D CSD but *not* from the data measured in the real grain pattern. In other words, using the S-model over the data from a polyhedral grain structure can not give a correct conversion. In particular, the excess small intercepts in 1D GSD over CSD will be automatically considered as being from small circles by the S-model, thus a larger number of small spherical grains than really exist is needed for the S-model in order to obtain the larger frequency of small intercepts, and so that a large number of ghost grains as to be seen in Fig. 1b will be given by the S-model.

The physical reason for this discrepancy can easily be located, if one considers the fact that much fewer small intercepts can be obtained during the measurement on a spherical (circular) pattern than on a polyhedral grain pattern, since, in contrast to the supposition of the S-model, grains possess corners and edges. In order to give a quantitative analysis, a new 2D polygonal grain model has been developed, which will be given in the following.

For the sampling probability $q_{12}^{P}(R)$, i.e. the probability that a polygonal grain with size R is met by a straight measuring line is determined by the length $2R_{Pr}$ obtained by the projection of the polygon onto the line normal N_T of the measuring line $\boldsymbol{T}$, (see Fig. 3), which can be calculated by integrating $\cos\theta\, ds$ along the whole perimeter of the polygon and averaging over all measuring directions:

$$q_{12}^{P} = 2\overline{R}_{Pr} = \frac{1}{2\pi}\int_{-\pi/2}^{\pi/2}\oint_{s}\cos\theta\, ds\, d\theta = \frac{s}{\pi} \tag{4}$$

It is clear that for circular grains, since $s=2\pi R$, Eq.(4) gives the same result as Eq.(3). To find a relationship between R and s for polygonal grains (irregular polygons), the perimeters s, side-numbers n and grain radii R of about 2700 grains of various 2D annealed metallic samples with about

equiaxed grain patterns have been measured, averaged in grain size classes, and plotted in Fig. 4 with solid dots. Using the least square method these results can be represented by the linear form:

$$s = \pi(2.1R + 0.21\overline{R}) \tag{5}$$

This is plotted in Fig. 4 (solid line) and leads to the sampling probability of polygons:

$$q_{12}^{P}(R) = \frac{s}{\pi} \approx 0.21\overline{R} + 2.1R \tag{6}$$

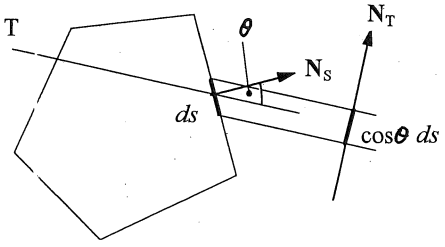

Fig. 3 calculating the sampling probability of a polygon

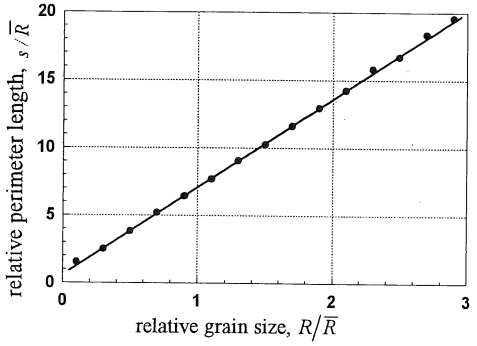

Fig. 4 perimeter lengths as a function of grain sizes in 2D

The truncation effect is strongly dependent upon the geometric feature of the grain. Some given geometric model is therefore necessary to calculate the truncation probability. In the present paper the regular pentagon, hexagon and heptagon have been used, since they are simple and also close to the most 2D grains geometrically. The calculation has been done analytically with the method described in the following for pentagon as an example.

As shown in Fig. 5 for a pentagon with the side length a, the intercept length L of a measuring line T through the pentagon are determined by the orientation angle φ and the distance Z between the measuring line and the coordinate origin:

$$L(\varphi, Z) = \begin{cases} \left(\cot\varphi + \cot(2\omega - \varphi)\right)Z & , \quad 0 < Z \le Z_1(\varphi) \\ \dfrac{2(Z - a\cdot\sin\varphi)\sin}{\cos(2\varphi) + \cos\omega} + \dfrac{a\cdot\sin(3\omega)}{\sin(2\omega - \varphi)} & , \quad Z_1(\varphi) < Z \le Z_2(\varphi) \end{cases} \tag{7}$$

with $\omega = \pi/5$ and

$$\begin{cases} Z_1(\varphi) = a \cdot \sin\varphi \\ Z_2(\varphi) = a \cdot \sin\varphi + a\left(1 - \dfrac{\sin\varphi}{\sin(2\omega - \varphi)}\right)\cos\left(\dfrac{\pi}{10} + \varphi\right) \end{cases} \tag{8}$$

For an arbitrary constant λ, ($0<\lambda\leq 2a\cos\omega$), the equation $L(\varphi,Z)=\lambda$ gives one curve when $0<\lambda\leq a$ or two curves when $\lambda>a$ in the $a\sim Z$ plane by Eq.(7). The length of these curves is proportional to the truncation probability of the pentagon with the intercept length λ:

$$p^{\text{Pent}}(a,\lambda) = C \cdot S_{L=\lambda} = C \int_{L=\lambda} \sqrt{1+\left(dZ/d\varphi\right)^2}\, d\varphi \tag{9}$$

This linear integration is then numerically calculated and normalized to determine the constant C. For the application the function $p^{\text{Pent}}(a,\lambda)$ is transformed into $p^{\text{Pent}}(R,r)$ by replacing a and λ with $r=\lambda/2$ being the 1D radius and R the equivalent radius of the pentagon respectively.

The calculation of the truncation effect of a hexagon or heptagon is similar although more complicated since they have more sides than a pentagon. The results are given in Fig. 6.

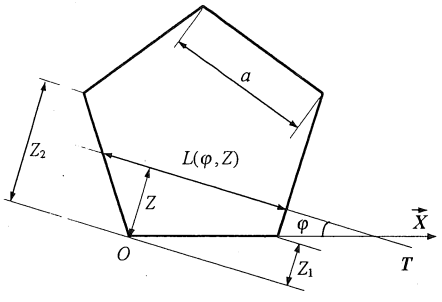

Fig. 5 the intercept length of a line through a pentagon

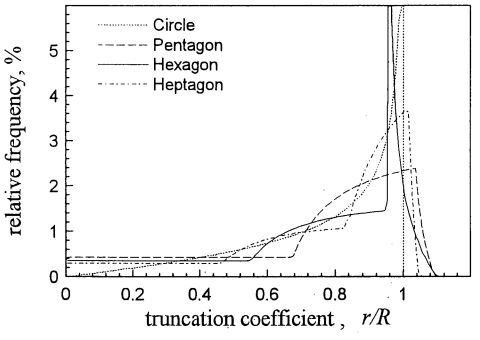

Fig. 6 truncation probabilities for some regular polygons as compared with circle

From Fig. 6 one sees that: (i) the curve for hexagon has a sharp peak at $r/R\approx 0.95$, which is directly originated from the parallel sides of the hexagon, (also the curve for circle has sharp peak at

$r=R$, since a circle has infinite infinitesimal parallel sides); (ii) the curves of the polygons extend through to the region of $r/R>1$; and (iii) the curves of polygons start not from $p=0$ but from $p>0$ at $r/R=0$

Since real 2D grains are not regular heptagons, hexagons or heptagons, some modification must be made to make the model to be in conformity with the feature of real grain structures. For this reason, the 2D SDFs are converted from 1D SDF of the NiAl sample (Fig. 1a) with the S-model (Circle), Pentagon-, Hexagon-, Heptagon-model and the regular Polygons-model*, which is defined by the average of the 3 polygons above, and plotted in Fig. 7. Here one sees that the 2D SDFs calculated with various polygonal models are very close to each other (and also very close to the measured 2D SDF), while the SDF calculated with the S-model contains much more small grains than others.

From this result one would be able to recognize that for the truncation effect the most important difference between the S-model and a polygonal grain model would be in the region of small r/R, i.e., as one can see from Fig. 6, the truncation probability curves of polygons start from constants while the S-model from 0 at $r/R=0$ and the differences in the large r/R region would be not principle. Therefore we can make a radical modification on the RP-model to develop a simple polygonal grain model. Such a model has been so chosen: firstly the $p(R,r)$ for small

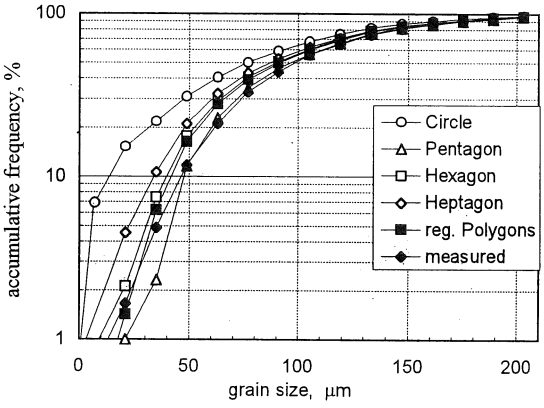

Fig. 7 2D SDFs calculated from 1D with various models

* For all polygonal models, the truncation probability is defined by Eq.(6).

r/R should be constant with the value similar to the Hexagon since the angle at the corners of grains, which determine the $p(R,r)$ for small r/R, will often be close to 120° independent of the number and length of sides of the grain; and secondly, the $p(R,r)$ for large r/R can be similar to the S-model since the difference of various models in this region plays only a little role on the conversion; thirdly, the $p(R,r)$ near r/R=1 should be limited since there would be few parallel sides in a real grain structure; and finally, the $p(R,r)$ would be stopped at r/R=1 for the sake of simplifying the conversion process. Thus a new geometrical model called the Polygonal model (P-model) has been defined with the sampling probability given by Eq.(6) and the truncation probability by:

$$p_{12}^{P}(R,r)R=\begin{cases}0.36 & , \quad (0.00<r/R\le 0.34)\\ r/\sqrt{R^2-r^2} & , \quad (0.34<r/R\le 0.95)\\ 5.0 & , \quad (0.95<r/R\le 1.00)\\ 0.0 & , \quad (1.00<r/R)\end{cases} \tag{10}$$

Fig. 8 gives the truncation probabilities $p_{12}(R,r)$ of the S-, the RP- and the P-model. To check these models experimentally, three samples are used in the present paper, they are: (i) Al-3%Mg with 1260 measured 2D grains, (ii) Armco-Iron with 700 grains, and (iii) NiAl with 780 grains (Fig. 1a). From the 1D grain size measured data, the 2D SDFs are converted using various models, the average 2D grain radii $\overline{R}$ and the variation coefficients κ(defined by the ratio of the standard deviation of grain sizes to the average grain size, $\kappa=\sigma/\overline{R}$) are then calculated and exhibited in Table 1 as compared with the experimentally measured 2D data. Here one sees that the relative deviations of the calculated values from the measured ones are about 30 % in $\overline{R}$ and over 40% in κ for the S-model, but smaller than 10% for both RP- and P-models.

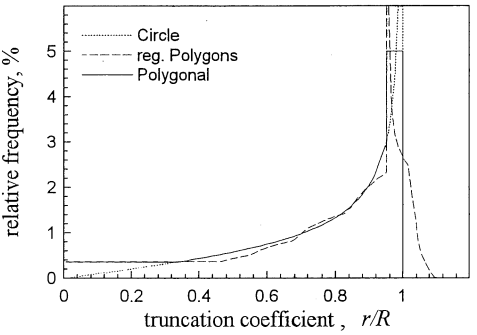

Fig. 8 truncation probabilities of various 2D models

Table 1 Comparison on the 2D average radii $\overline{R}$ and variation coefficients κ

	average radius $\overline{R}$, μm				variation coefficient κ			
	measured	S-model	RP-model	P-model	measured	S-model	RP-model	P-model
Al-3%Mg	16.29	10.64	15.11	15.15	0.54	0.84	0.58	0.58
Armco-Fe	17.51	11.34	16.73	16.75	0.68	0.95	0.70	0.69
NiAl	47.55	33.78	45.90	45.66	0.44	0.73	0.49	0.49

These results would be a great surprise since the P-model is only a rough approximation and is nearly as simple as the S-model, but leads to such a good agreement, as compared with the S-model, between the converted and the measured data. Because the principle difference between the P- and S-model is only that $p_{12}(R,r)$ tends to a constant for the P-model but to zero for the S-model when $r \to 0$, the results above indicates that the error caused by the S-model lies in the fact that, in contrast to spheres, real grains posses corners (and edges in 3D) near to which the probability of obtaining small intercept lengths is strongly increased.

3. Development of the Polyhedral model

The sampling probability that a polyhedron is met by a measuring line or a measuring plane, i.e. q_{13} or q_{23}, is given by the average projection area $\overline{A}_{Pr}$ or the average projection height $\overline{H}_{Pr}$ of the polyhedron respectively. Because it is extremely difficult to estimate both $\overline{A}_{Pr}$ and $\overline{H}_{Pr}$ for real grains, and also being considered the fact that the sampling effect of the P-model is only some modification of that of the S-model, see Eq.(3) and Eq.(6), an approximate method was used here to find the expressions of the sampling probabilities of polyhedral grain in 3D.

For q_{13}, the average projection area $\overline{A}_{Pr}$ can be expressed by the size R and the face number N for regular polyhedrons with $N = 4$, 6, 8, 12, 20, etc. with the data of any mathematical handbook. Using the results of measurements of R and N for various grain samples [17], q_{13} can then be given with the function of grain size R :

$$q_{13}(R) = \overline{A}_{Pr} = 3.1R^2 + 0.42\overline{R}R \tag{11}$$

For q_{23}, if we consider the fact that on the projection plane perpendicular to the measuring plane the configuration of the polyhedron and the measuring plane is reduced to a polygon and a line, q_{23} can be then approximately replaced by q_{12}, that is:

$$q_{23}(R) = q_{12}(R) = 2.1R + 0.21\overline{R} \tag{12}$$

To calculate the truncation probabilities of a polyhedral grain cut by a measuring line or a plan, p_{13} or p_{23}, one should pay the most attention to the small intercepts or intersects, while their distributions in large r/R region will be less significant for the conversion quality, as we just discussed in the 2D case. Hence, for the calculation of the truncation probabilities, we choose here the 14-sided tetrakaidecahedron (Fig. 9), since its geometry is not only simple but also very similar to real grains. Especially, the angles between two faces of the tetrakaidecahedron are very close to that of a grain, which is a very important geometrical feature for the truncation probabilities.

Because it is very complicated (if not impossible) to calculate $p(R,r)$ analytically like in the 2D case, a numerical method has been used in the present work. Using a large number of random measuring lines or planes across the tetrakaidecahedron (Fig. 9) with the efficient radius of R, the distributions of intercept length and intersect area can be calculated respectively, which give p_{13} and p_{23}. The results were plotted in Fig. 10 (dot-dash lines) together with the curves of the S-model (dash lines).

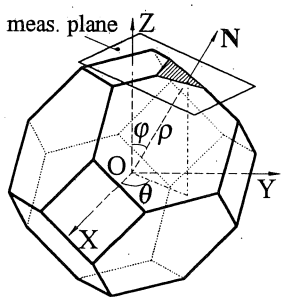

Fig. 9 a measuring plane intersects the tetrakaidecahedron

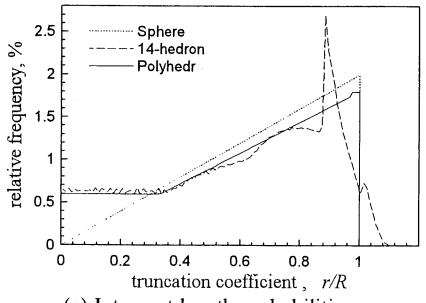

(a) Intercept length probabilities p_{13}

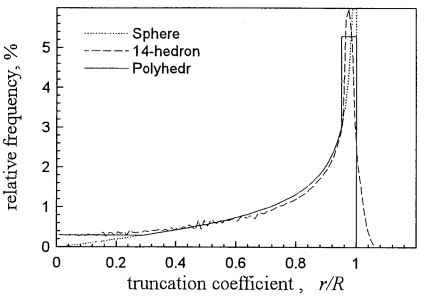

(b) Intersect area probabilities p_{23}

Fig. 10 Truncation probabilities of the S-, K- and P-model

Since the tetrakaidecahedron has many parallel faces, the resulting curves contain sharp peaks at $r \approx 0.89R$ for 1D→3D and $r \approx 0.96R$ for 2D→3D. Also here calculations with bodies without parallel faces would have been beneficial, but are very complicated. According to the discussion in the 2D case, we can further simplify the model to cut the peaks without decreasing the conversion quality of the calculated SDFs. The simplification of the truncation probabilities was so carried out that first the simple expressions for p_{13} and p_{23} should be obtained, second the simplified functions must be well fitted with the data from the tetrakaidecahedron, and at last the truncation effect with $r>R$ will be neglected to simplifying the converting process later. As the result the following set of truncation functions is proposed, which is called as Polyhedron-model, or simply "P-model" in the present work and also plotted in Fig. 10 (solid lines).

$$p_{13}^{P}(R,r)R = \begin{cases} 0.60 & , \quad (0.00 < r/R \le 0.33) \\ 1.80\ r & , \quad (0.33 < r/R \le 0.97) \\ 1.80 & , \quad (0.97 < r/R \le 1.00) \\ 0 & , \quad (1.00 < r/R) \end{cases} \tag{13}$$

$$p_{23}^{P}(R,r)R = \begin{cases} 0.31 & , \quad (0.00 < r/R \le 0.30) \\ r/\sqrt{R^2 - r^2} & , \quad (0.30 < r/R \le 0.95) \\ 5.3 & , \quad (0.95 < r/R \le 1.00) \\ 0.0 & , \quad (1.00 < r/R) \end{cases} \tag{14}$$

4. Experiments and discussions

For the direct check of various geometrical models, a block of extremely coarse grain-sized high pure aluminium was separated into single grains with the method of forming a Al-Ga liquid alloy film in grain boundaries. The grain sizes were then obtained from the weights of the grains, and the experimental 3D SDF was calculated from about 1000 single grains. From the section planes of the same sample, 1D SDF was measured and converted into 3D using the S- and P-models respectively. In Fig 11(a), the 3D SDFs converted with the S-model (open circles) and with the P-model (open squares) are plotted to compare with the measured 3D SDF (close diamonds).

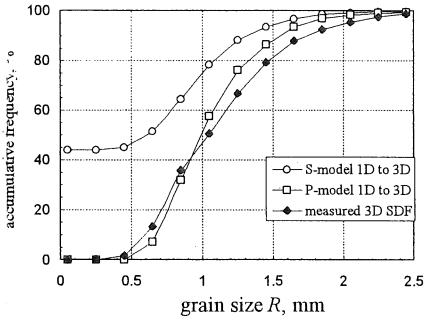

(a) high-pure aluminium sample

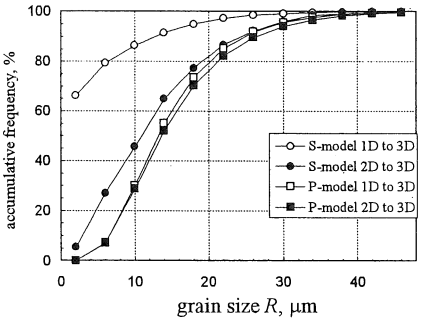

(b) Al-3%Mg sample

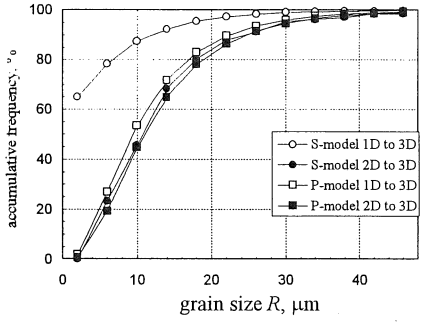

(c) Armco pure Iron sample

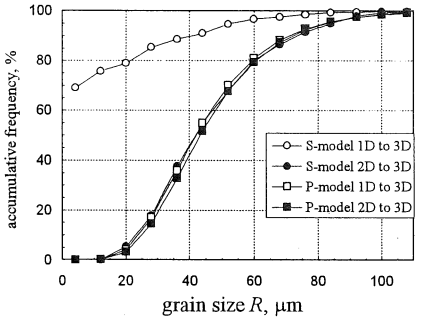

(d) ordered NiAl sample

Fig. 11 Comparison of the 3D SDFs converted from 1D with the directly measured (a) or from 2D converted ones (b, c, d) for the S- and P-models

Due to the difficulty of direct measurement of 3D SDFs, the further experimental check of the S- and P-model has been made by the comparison of 3D SDFs converted from 1D and 2D SDFs measured from the same sample, since only when both 3D SDFs are coincident the geometrical model used can be valid. In Fig. 11, 3D SDFs converted from 1D (open symbols) and from 2D (close symbols) using the S-model (circles) and P-model (squares) for Al-3%Mg (b), Armco-Fe (c) and the ordered NiAl (d) are plotted.

From Fig. 11 one sees that the 3D SDFs converted from 1D using the S-model are very different from the measured 3D SDF or the 3D SDFs converted from 2D. The common and significant feature of the 3D SDFs calculated from 1D with the S-model is that they contain much more small grains than the measured or from 2D converted 3D SDFs. The origin of such systematical error, as we just discussed in the 2D case in section 2 of the present paper, is that *Spheres* possess no edges and corners and so that the S-model consider the most small intercepts measured from the grain edges or corners as from small spherical grains.

Because the conversion of 1D to 3D can be principally divided into one 1D to 2D and one 2D to 3D conversions, the systematic error of the S-model will be introduced twice for 1D to 3D conversion and much larger than that from 1D to 2D or 2D to 3D conversion (*cf.* Fig. 7 and Fig. 11). With this view, a 3D SDF converted from 1D by the S-model could be useless even for a rough estimation of grain sizes. In the other side, one finds from Fig. 11 that the P-model gives the 3D SDFs practically identical with the measured one even directly converted from 1D, and also the 3D SDFs from 1D and 2D are coincident, which means that the P-model is a rather proper geometrical simplification of the calculation of 3D SDFs from the measurements of 1D or 2D.

4. Conclusions

The so far applied method of calculating 3D grain size distributions from 1D linear intercept and 2D intersect area distributions assumes spherical grain shape. This method has the advantage of great simplicity, but leads to a grave systematic error, which is mainly due to the absence of edges or corners in spheres being present in polyhedral grains. In the present paper it has been demonstrated that the use of a properly chosen polyhedral grain model is nearly as simple as the so far used spherical grain model, but gives much better results. Particularly the here proposed "P-model" yields very good conversion from 1D to 3D and 2D to 3D and very well suited for practical application in calculating of 3D grain size distributions from 1D or 2D distributions.

Acknowledgments

The authors like to thank Dr. I. Heckelmann for many helpful discussions. The work is financially supported by the State Education Commission of China and dem Deutschen Akademischen Austauschdienst (DAAD).

References

[1] R.T. DeHoff : Quantitative serial sectioning analysis: preview, *J. Microsc.*, V.**131**, p.259~263, (1983).

[2] F. N. Rhines, K. R. Craig, et al. : Measurement of average grain volume and certain topological parameters by serial section analysis, *Metall. Trans.*, V.7A, p.1729~1734, (1976).

[3] S. D. Wicksell : The corpuscle problem. A mathematical study of a biometric problem, *Biometrika*, V.**17**, p.84~99, (1925).

[4] E. Scheil : Die Berechnung der Anzahl und Größenverteilung kugelförmiger Kristalle in undurchsichtigen Körper mit Hilfe der durch eine ebenen Schnitt erhaltenen Schnittkreise, *Z. anorg. Chem.*, V.**201**, p.259~264, (1931).

[5] E. Scheil : Statistische Gefügeuntersuchungen I., *Z. Metallkde.*, V.**27**, p.199~209, (1935).

[6] H. E. Exner : Analysis of grain- and particle-size distributions in metallic materials, *Intern. Metall. Reviews*, V.**17**, p.25~42, (1972).

[7] R. T. DeHoff and F. N. Rhines : *Quantitative Microscopy,* New York and London, (1968).

[8] S. A. Saltykov : The determination of the size distribution of particles in an opaque material from measurement of the size distribution of their sections, *Stereology,* Springer-Verlag New York Inc., New York, p.163~173, (1967).

[9] G. Bockstiegel : Eine einfache Formel zur Berechnung räumlicher Größenverteilungen aus durch Linearanalyse erhaltenen Daten, *Z. Metallkde.*, V.**57**, p.647~652, (1966).

[10] H. E. Exner : Modellversuche zu den Umrechnungsverfahren von linearen und ebenen in räumliche Größenverteilungen, *Metall*, V.**21**, p.431~438, (1967).

[11] L.-M. Cruz Orive : Particle size-shape distributions: the general spheroid problem. I. Mathematical model, *J. Microsc.*, V.**107**, p.235~253, (1976).

[12] L.-M. Cruz Orive : Particle size-shape distributions: the general spheroid problem. II. Stochastic model and practical guide, *J. Microsc.*, V.**112**, p.153~167, (1978).

[13] R. T. DeHoff : The determination of the size distribution of ellipsoidal particles from measurements made on random plane section, *Trans. Metall. Soc. AIME*, V.**224**, p.474~477, (1962).

[14] H. E. Exner : Analyse der Größenverteilung von Körnern, Poren und Pulverteilchen, *Z. Metallkde.*, V.**57**, p.755~763, (1966).

[15] N. V. Naumovich : Statistical parameters of some polyhedrons, *Pract. Metallography*, V.**17**, p.192~200, (1980).

[16] X. B. Zhao, Z.Y. Chen : A new method for calculating spatial grain size from the measurements made on random plane sections, *J. Comp.-Ass. Microsc.*, V.**5**, p.257~263, (1993).

[17] R.T. DeHoff : Quantitative serial sectioning analysis: preview, *J. Microsc.*, V.**131**, p.259~263, (1983).

Received:20 July 1997 *Accepted:23 March 1998*